AEROELASTIC ANALYSIS FOR HELICOPTER ROTOR BLADES IN HOVER AND FORWARD FLIGHT

In Lee*, Min-Soo Jeong*, Seung-Jae Yoo**
***KAIST, Daejeon, Korea, ****Hyundai Heavy Industries, Co., Ltd., Ulsan, Korea**
inlee@kaist.ac.kr; ms_jeong@kaist.ac.kr; sjryu1004@hhi.co.kr

Keywords: *Aeroelasticity, Freewake, Helicopter, Hover, Forward flight*

Abstract

Aeroelastic characteristics considering wake effects for helicopter rotor blades in hover and forward flight were investigated. To take into account the large deformations of rotor blades, a large deflection beam model was used. Also, to estimate unsteady wakes and calculate its induced velocities, a freewake model was applied. The aerodynamic forces of the rotor blades were obtained by using a vortex lattice method (VLM) in hover and forward flight. In the case of the hovering flight, Newton-Raphson iterative method was applied to the aeroelastic analysis to obtain the numerical solutions for steady-state blade deflections. The flap, lag, and torsion deflections considering wake effects by using the freewake model were investigated. The p-k method in the frequency domain was used to predict the lag damping and frequency, which are directly relevant to the dynamic stability of helicopter rotor blades. The numerical results were compared to the experiments and the ones using a two-dimensional quasi-steady model with a uniform inflow model. For the forward flight, nonlinear periodic blade responses were obtained by integrating the full finite element equation in time through a coupled procedure with a vehicle trim. After the periodic blade deflections were obtained, the stability analysis was performed for the linearlized stability equations with a Floquet transition matrix. The numerical results using the freewake model were compared to the ones using the two-dimensional quasi-steady model.

1 Introduction

Several helicopter accidents reportedly occur when the aircraft is cruising [1]. The helicopter is frequently put at risk by an unstable and complicate flow field. Unsteady wakes are generally generated by rotary wings. The flow field around the helicopter rotor blades is tremendously complicated. For these reasons, the helicopter is subjected to a strict vibratory environment because of the unsteady wakes. Thus, aeroelastic analysis that predicts the vibratory stability of rotor blades is a highly aspect of helicopter research and lots of studies for dynamic stability analysis have been implemented [2-7].

In most studies on the aeroelastic responses of helicopter rotor, nonlinear beam models are applied to describe one-dimensional large deformations and rotations. Helicopter rotor blades are usually modeled as one-dimensional beam since this approach is able to reduce the computational cost. Nonlinear beam models with one-dimensional global deflections are generally classified in terms of two types of beam theory. One is the moderate deflection beam theory based on ordering schemes. This theory has been applied to most rotor blade structural models [8-11]. The other is the large deflection beam theory [12-13] and this theory use of Euler angles without any artificial restrictions. Aeroelastic analysis requires the interaction of aerodynamic forces with structural characteristics. A two-dimensional aerodynamic model that is essentially based on Greenberg's theory [14] has been applied to most aeroelastic models as a way of reducing the computational time and simplifying the aeroelastic model [15-20]. However, the two-dimensional aerodynamic model has limitations with regard to wake effects. Wake models, on

the other hand, have become popular in three-dimensional aerodynamic models where wake effects are taken into account in the aeroelastic analysis. A freewake model is one of the wake models that overcome these limitations [21-22].

For aeroelastic simulation, in this study, a large deflection beam model, which considers the nonlinear behavior of the helicopter rotor blades, was used to the structural model. Also, the wake effects were accounted for by using the freewake method. The stability analyses in hover and forward flight have been performed, and the damping results were considerably affected by the wake effects.

2 Governing Equations

2.1 Deflections for the Equilibrium State

The governing equation for the equilibrium state requires that the following parameters be defined: the kinetic energy, the strain energy, and the virtual work of external forces. The kinetic energy, δT, the strain energy, δU, and the virtual work, δW, for a rotating cantilever beam can be expressed as follows:

$$\delta T = \int_0^l \int_A \rho \{\delta V\}^T \{V\} \mathrm{d}A\mathrm{d}x_1 , \quad (1)$$

$$\delta U = \int_0^l \begin{Bmatrix} \delta\bar{e} \\ \delta\bar{\kappa} \end{Bmatrix}^T \begin{bmatrix} \mathbf{A} & \mathbf{B} \\ \mathbf{B}^T & \mathbf{D} \end{bmatrix} \begin{Bmatrix} \bar{e} \\ \bar{\kappa} \end{Bmatrix} \mathrm{d}x_1 , \quad (2)$$

$$\delta W = \int_0^l \int_A \{\delta R\}^T \{f\} \mathrm{d}A\mathrm{d}x_1 , \quad (3)$$

where a vector of velocity $\{V\}$ is defined by the elastic blade velocity on the rotating coordinates and the velocity of the coordinate rotation; $\{\delta\bar{e}\}$ and $\{\delta\bar{\kappa}\}$ represent the strain and moment strain at the elastic axis, respectively; $\mathbf{A}$, $\mathbf{B}$, and $\mathbf{D}$ are 3 * 3 matrices which depend on the material properties and geometry of the cross section; $\{\bar{f}\}$ is the aerodynamic force vector; and δT, δU, and δW are extended by means of the transformation matrix $\mathbf{T}(x_1)$ [13,20]. When δT, δU, and δW are substituted in Hamilton's principle, the governing equation can be defined as follows:

$$\mathbf{M}(q)\{\ddot{q}\} + \mathbf{G}(q)\{\dot{q}\} + \mathbf{P}(q) - \mathbf{P}_\mathrm{C}(q) - \mathbf{P}_\mathrm{A}(q) = 0 \quad (4)$$

where $\mathbf{M}(q)$ is the mass matrix, $\mathbf{G}(q)$ is the gyroscopic matrix, $\mathbf{P}(q)$ is the internal elastic force vector, $\mathbf{P}_\mathrm{C}(q)$ is the centrifugal load vector, and $\mathbf{P}_\mathrm{A}(q)$ is the converged steady aerodynamic force vector. The aeroelastic stability can be estimated on the basis of the equilibrium state. On the assumption of an equilibrium state, Eq. (4) can be simplified by ignoring the time-dependent terms as follows:

$$\mathbf{f}(q) = \mathbf{P}(q) - \mathbf{P}_\mathrm{C}(q) - \mathbf{P}_\mathrm{A}(q) = 0 . \quad (5)$$

Using the Taylor series extension, Eq. (5) can be rewritten as follows as a relation between stiffness and force:

$$\begin{aligned} &\left[\mathbf{K}_\mathrm{T}^{(i-1)} - \mathbf{K}_\mathrm{C}^{(i-1)} - \mathbf{K}_\mathrm{A}^{(i-1)}\right]\left\{\Delta q^{(i)}\right\} \\ &\quad = -\mathbf{P}\left(q^{(i-1)}\right) + \mathbf{P}_\mathrm{C}\left(q^{(i-1)}\right) + \mathbf{P}_\mathrm{A}\left(q^{(i-1)}\right) \end{aligned} , \quad (6)$$

where

$$\mathbf{K}_\mathrm{T}^{(i-1)} = \left.\frac{\partial \mathbf{P}}{\partial q}\right|_{q^{(i-1)}} , \quad \mathbf{K}_\mathrm{C}^{(i-1)} = \left.\frac{\partial \mathbf{P}_\mathrm{C}}{\partial q}\right|_{q^{(i-1)}} , \quad \mathbf{K}_\mathrm{T}^{(i-1)} = \left.\frac{\partial \mathbf{P}_\mathrm{A}}{\partial q}\right|_{q^{(i-1)}} ,$$

where $\mathbf{K}_\mathrm{T}^{(i-1)}$, $\mathbf{K}_\mathrm{C}^{(i-1)}$, $\mathbf{K}_\mathrm{A}^{(i-1)}$ are the tangential, centrifugal and tangential aerodynamic matrix, respectively. The aeroelastic deflections on the equilibrium state can be obtained by using the Newton-Raphson iterative method in Eq. (6).

2.2 Stability Analysis in Hover

The aerodynamic model based on Greenberg's theory [14] was combined with the unsteady aerodynamics based on the freewake model for the purpose of analyzing the dynamic stability. The aerodynamic forces and moment are defined as follows:

$$P_S = L' \sin\alpha - D_0 \cos\alpha + L_{UC} \sin\alpha , \quad (7)$$

$$P_N = L' \cos\alpha + D_0 \sin\alpha + L_{UC} \cos\alpha + L_{NC} , \quad (8)$$

$$M = M_\theta + M_{UC} + M_{NC} , \quad (9)$$

The unsteady aerodynamics can be written as follows:

$$L_{UC} = a_0 \rho_a U b C(k)\left[-U_P{}^t + b\left(\frac{1}{2}-a\right)\dot{\varepsilon}\right], \quad (10)$$

$$L_{NC} = \frac{1}{2} a_0 \rho_a b^2 \left[-\dot{U}_P - ba\ddot{\varepsilon}\right], \quad (11)$$

$$M_{UC} = a_0 \rho_a U b^2 \left(a+\frac{1}{2}\right) C(k)\left[-U_P{}^t + b\left(\frac{1}{2}-a\right)\dot{\varepsilon}\right], \quad (12)$$

$$M_{NC} = \frac{1}{2} a_0 \rho_a b^2 \left[-ba\dot{U}_P - \frac{1}{2} U b\dot{\varepsilon} - b^2\left(\frac{1}{8}+a^2\right)\ddot{\varepsilon}\right], \quad (13)$$

where $\dot{\varepsilon}$ is the angular velocity, b stands for the half value of the chord length, a indicates the elastic axis position, and $C(k)$ is the Theodorsen lift deficiency function.

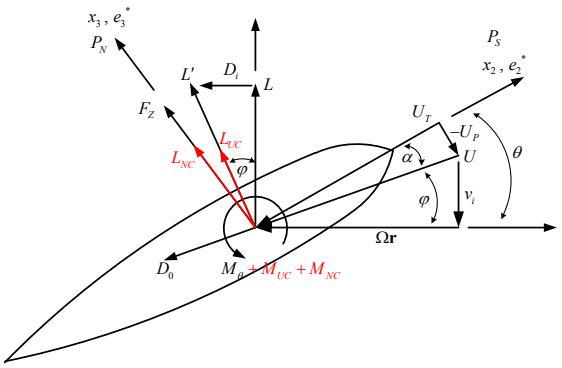

Fig.1 Sectional aerodynamics of the rotor blade

The induced velocity according to the freewake model was employed to calculate the lift deficiency function. The steady and unsteady aerodynamic forces and moments are shown in Fig. 1. Then, Eq. (3) can be rewritten as follows:

$$\frac{\delta W}{m_0 \Omega^2 R^3} = \int_0^1 \begin{Bmatrix} \delta\bar{u} \\ \delta\alpha \end{Bmatrix}^T \left[-\frac{\gamma\bar{c}}{24}\begin{bmatrix} \bar{A}_M \end{bmatrix} \begin{Bmatrix} \ddot{\bar{u}} \\ \ddot{\alpha} \end{Bmatrix} \frac{1}{\Omega^2} + \frac{\gamma}{6}\begin{bmatrix} \bar{A}_C \end{bmatrix} \begin{Bmatrix} \dot{\bar{u}} \\ \dot{\alpha} \end{Bmatrix} \frac{1}{\Omega} + \frac{\gamma}{6}\begin{Bmatrix} \bar{A}_f \end{Bmatrix} \right] d\bar{x}_1, \quad (14)$$

$$\mathbf{M}_\mathbf{A}(q) = \int_0^1 \mathbf{H}^T \left[-\frac{\gamma\bar{c}}{24}\begin{bmatrix} \bar{A}_M \end{bmatrix} \right] \mathbf{H} d\bar{x}_1, \quad (15)$$

$$\mathbf{G}_\mathbf{A}(q) = \int_0^1 \mathbf{H}^T \left[\frac{\gamma}{6}\begin{bmatrix} \bar{A}_C \end{bmatrix} \right] \mathbf{H} d\bar{x}_1, \quad (16)$$

$$\mathbf{P}_\mathbf{A}(q) = \frac{\gamma}{6}\int_0^1 \mathbf{H}^T \begin{Bmatrix} \bar{A}_f \end{Bmatrix} d\bar{x}_1, \quad (17)$$

where $\mathbf{M}_\mathbf{A}$ is the aerodynamic mass matrix, $\mathbf{G}_\mathbf{A}$ is the aerodynamic damping matrix, and $\mathbf{P}_\mathbf{A}$ is the steady aerodynamic force vector. Using Eqs. (1, 2) and Eq. (14), the governing equation can be written as follows:

$$\frac{1}{\Omega^2}\mathbf{M}(q_0)\ddot{\tilde{\mathbf{q}}}(t) + \frac{1}{\Omega}\mathbf{G}(q_0)\dot{\tilde{\mathbf{q}}}(t) + \mathbf{K}(q_0)\tilde{\mathbf{q}}(t) - \mathbf{A}(q_0,k)\tilde{\mathbf{q}}(t) = 0, \quad (18)$$

where

$$\mathbf{A}(q_0,k) = \mathbf{A}_\mathbf{R} + i\mathbf{A}_\mathbf{I} = \int_0^1 \mathbf{H}^T \left\langle \frac{\gamma\bar{c}}{24}\left(\frac{2\bar{r}}{\bar{c}}\right)^2 k^2 \begin{bmatrix} \bar{A}_M \end{bmatrix} - \frac{\gamma}{6}\left(\frac{2\bar{r}}{\bar{c}}\right) k \begin{bmatrix} \bar{A}_C{}^I \end{bmatrix} \right\rangle \mathbf{H} d\bar{x}_1 + i\int_0^1 \mathbf{H}^T \left\langle \frac{\gamma}{6}\left(\frac{2\bar{r}}{\bar{c}}\right) k \begin{bmatrix} \bar{A}_C{}^R \end{bmatrix} \right\rangle \mathbf{H} d\bar{x}_1 \quad (19)$$

The p-k method is applied with the normal mode method. Then, the governing equation can be linearized as follows:

$$\left\langle \begin{bmatrix} \mathbf{K}_\mathbf{I} & \mathbf{G}_\mathbf{I} \\ 0 & \mathbf{I} \end{bmatrix} - \bar{p}\begin{bmatrix} 0 & -\underline{\mathbf{M}} \\ \mathbf{I} & 0 \end{bmatrix} \right\rangle \begin{Bmatrix} y \\ \dot{y} \end{Bmatrix} = \begin{Bmatrix} 0 \\ 0 \end{Bmatrix}, \quad (20)$$

where

$$\{\tilde{q}(t)\} = [\Phi]\{y(t)\}, \quad (21)$$

$$(\mathbf{a}_\mathbf{R} + i\mathbf{a}_\mathbf{I}) = [\Phi]^T (\mathbf{A}_\mathbf{R} + i\mathbf{A}_\mathbf{I})[\Phi], \quad (22)$$

$$y(t) = e^{pt} y, \quad p = \lambda + i\omega, \quad \bar{p} = p/\Omega, \quad (23)$$

$$\mathbf{K}_\mathbf{I} = \underline{\mathbf{K}} - \mathbf{a}_\mathbf{R}, \quad (24)$$

$$\mathbf{G}_\mathbf{I} = \underline{\mathbf{G}} - \frac{1}{k}\left(\frac{\bar{c}}{2\bar{r}}\right)\mathbf{a}_\mathbf{I}. \quad (25)$$

The eigenvalue problem of Eq. (20) is solved, and the damping and frequency, which are related to the aeroelastic instabilities such as flutter, can be estimated.

2.3 Stability Analysis in Forward Flight

The periodic steady response is obtained using a time finite element approach [23]. The virtual energy for the Hamilton's weak form can be expressed as follows:

$$\int_{\psi_i}^{\psi_f} \delta y^T l d\psi = \delta y^T b\Big|_{\psi_i}^{\psi_f}, \quad (26)$$

where

$$\delta y = \begin{Bmatrix} \delta\dot{q} \\ \delta q \end{Bmatrix}, \quad l = \begin{Bmatrix} L_{\dot{q}} \\ L_q + Q \end{Bmatrix}, \quad b = \begin{Bmatrix} 0 \\ p \end{Bmatrix}, \quad (27)$$

where Q is the generalized force and L is the Lagrangian of the system. $L_{\dot{q}}$ and L_q are the partial derivatives of L with regard to generalized coordinates $\dot{q}$ and q, respectively, which are composed of displacements and angles, whereas $p = L_{\dot{q}}$ is the column vector of the generalized moment. ψ_i and ψ_f represent the initial and final states of time, respectively. Using a first-order Taylor-series of the left-hand side of Eq. (26) about a given state vector $\bar{y}$, the governing equation can be derived as follows:

$$\int_{\psi_i}^{\psi_f} \delta y^T l d\psi + \int_{\psi_i}^{\psi_f} \delta y^T \mathrm{K} \Delta \mathrm{y} d\psi = \delta y^T b \Big|_{\psi_i}^{\psi_f}, \quad (28)$$

where

$$\mathrm{K} = \begin{pmatrix} L_{\dot{q}\dot{q}} & L_{\dot{q}q} \\ L_{q\dot{q}} + Q_{\dot{q}} & L_{qq} + Q_q \end{pmatrix}, \quad (29)$$

where K is the local tangent matrix. Also, $L_{\dot{q}\dot{q}}$. $L_{\dot{q}q}$, L_{qq}, $Q_{\dot{q}}$ and Q_q indicate the second and first derivatives with respect to the subscripts, respectively. The time period for one revolution is discretized into a number of time elements with cubic variation. After assembling elements in a global system, a periodic boundary condition is imposed by folding the row and column of the assembled matrix and vector. The trim analysis is fully coupled with earlier blade steady response analysis to solve the blade response, pilot control inputs, and vehicle orientation simultaneously. The vehicle trim solution is calculated from the overall nonlinear vehicle equilibrium equations: three force equations and three moment equations.

For stability analysis, the blade perturbation equations of motion are linearized about the equilibrium position.

$$\begin{Bmatrix} \ddot{\tilde{q}} \\ \tilde{q} \end{Bmatrix} = \begin{pmatrix} L_{\dot{q}\dot{q}}(q_0) & L_{\dot{q}q}(q_0) \\ L_{q\dot{q}}(q_0) + Q_{\dot{q}}(q_0) & L_{qq}(q_0) + Q_q(q_0) \end{pmatrix} \begin{Bmatrix} \dot{\tilde{q}} \\ \tilde{q} \end{Bmatrix}, \quad (30)$$

where q_0 is the trim solution as a function of azimuth angle and $\tilde{q}(t)$ is small perturbation about the periodic equilibrium position. These equations include periodic coefficients and can be integrated in time for the proper initial conditions of displacements and velocities. The initial value of the perturbed blade motion is taken to be $0.1 * q_0$ at a proper time position. From the initial perturbation the blade is set free to move, and the blade perturbation equations of motion are integrated by the fourth-order Runge-Kutta method. To obtain more accurate modal damping and frequency, the initial perturbation of the blade is given only in the particular mode of interest [24].

3 Results

3.1 Aeroelastic deflections and aerodynamics

In this study, the freewake method was used to investigate the wake effects on the aeroelastic characteristics.

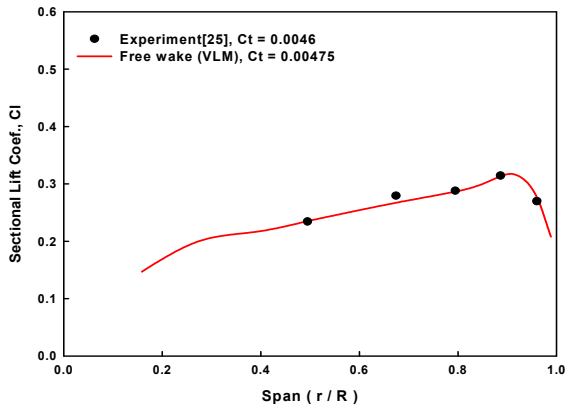

Fig.2 Sectional lift and thrust at pitch angle 8°

Fig. 2 shows the sectional lift computed with the freewake method based on VLM. The aspect ratio of the blade is about 6. The radius of the rotor is 3.75 ft and rotation speed at the tip is 491 fps. The blade was assumed to be rigid to ignore the elastic deformations, which means that the structural characteristics were not considered. The results were compared with measurement [25], and those results were good agreement with the experiment [25].

The lead-lag motion is generally sensitive and weak for the dynamic stability of helicopter rotor blades. For this reason, deflections in lead-lag mode were investigated. Isotropic rotor blades were modeled and analyzed. The rotor model is a two-bladed with a radius of 0.9615 m and a chord length of 0.0864 m. The structural

properties and the rotor parameter values are given in Table 1.

Table 1 Blade structural properties and rotor parameter values

Parameter	Blade set 1
Flap bending stiffness, EI_β	17.37 N-m2
Chord bending stiffness, EI_ζ	407.7 N-m2
Torsional rigidity, GJ	6.32 N-m2
Flap/ Lagwise moment of inertia, k_{m1}, k_{m2}	0 / 1.911×10^{-4} kg·m
Chordwise center of gravity	0.249 c
Elastic axis	0.254 c
Rotor speed, Ω	1000 rpm
Profile drag coefficient, C_{d0}	0.0079
Hub off-set ratio, e	0.1051
Lead-lag structural damping, ζ	0.00826
Lock number, γ	5.115

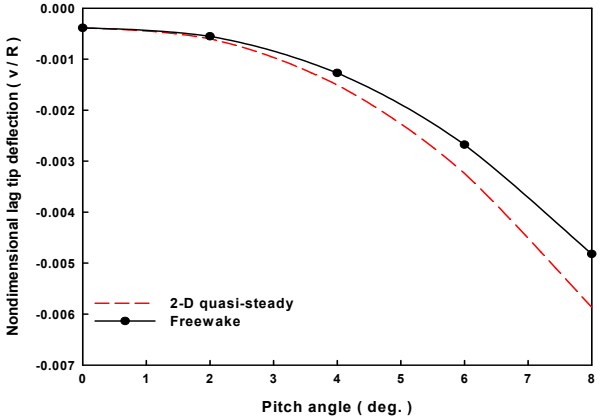

Fig.3 Non-dimensional lag tip deflections

Fig. 3 shows the non-dimensional lag tip deflections of the rotor blade. The deflections increased as the pitch angle increases and the deflections based on the freewake method were smaller than those based on the two-dimensional quasi-steady strip theory model. The offsets in the deflections of the freewake model and the two-dimensional quasi-steady model were resulted from the differences of the aerodynamic approach.

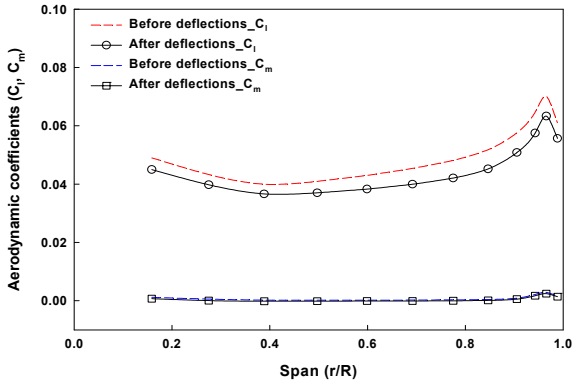

(a) Pitch angle of 2º

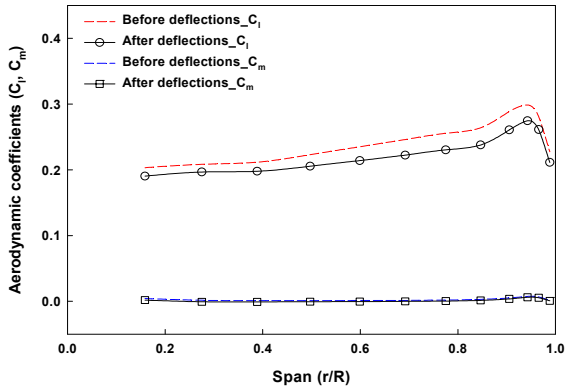

(b) Pitch angle of 4º

Fig.4 Lift and moment coefficients

Fig. 4 show the lift and pitching moment after the aeroelastic deflections at the pitch angles of 2 and 4 degrees. It is obviously found that the aerodynamic coefficients decrease due to the effect of the deflected blade.

3.2 Dynamic Stability in Hover

In most cases, the lag damping obtained from the freewake method was smaller than the result derived from the two-dimensional quasi-steady model. Newly developed aeroelastic module is devised in this study. In addition, not only the physical characteristics on the dynamic stability analysis but also the reliability of the results were investigated. Stability analysis of the blade model given in Table 1 was performed. Fig. 5 shows the lag damping of rotor blade. The damping values derived from the freewake model coincided with the experimental results [26] and those results were smaller than the results derived from the two-dimensional quasi-steady model.

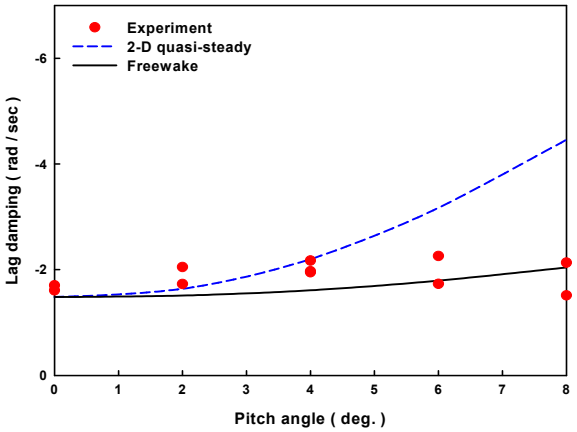

Fig.5 Lag damping values

Numerical results for two methods increased as pitch angle increases. Damping obtained from freewake method have similar tendency to measurements. Whereas, the discrepancies of lag damping between the two-dimensional quasi-steady model and experiments increased as the pitch angle increased. Also, the rotor blade is aeroelastically stable since the lag mode is negatively damped.

3.3 Dynamic Stability in Forward Flight

Four-noded cubic elements were used to model the period of one revolution. The properties of the vehicle and rotor are given in Table 2.

Table 2 Vehicle and structural properties

Main rotor	
Number of blades	4
Blade aspect ratio	0.055
Solidity, σ	0.07
Thrust level, C_T/σ	0.07
Lock number, γ	5.5
Lift curve, a_0	2π
Profile drag, C_{d0}	0.01
$EI_y/m_0\Omega^2R^4$	0.01080
$EI_z/m_0\Omega^2R^4$	0.02680
$GJ/m_0\Omega^2R^4$	0.00615
k_A/R	0.0290
k_{m1}/R	0.0132
k_{m2}/R	0.0247
Vehicle	
Longitude and latitude offset	0.0, 0.0
c.g. below hub, h/R	0.2
Flat plat area, $f/\pi R^2$	0.01

The present analysis used the full finite element method in the displacement-based formulation. Fig. 6 shows the flap and lag tip deflections of the baseline case for advance ratio of 0.3. The present results are compared with those of Ref. [27, 28], and the present results have similar trend with the references.

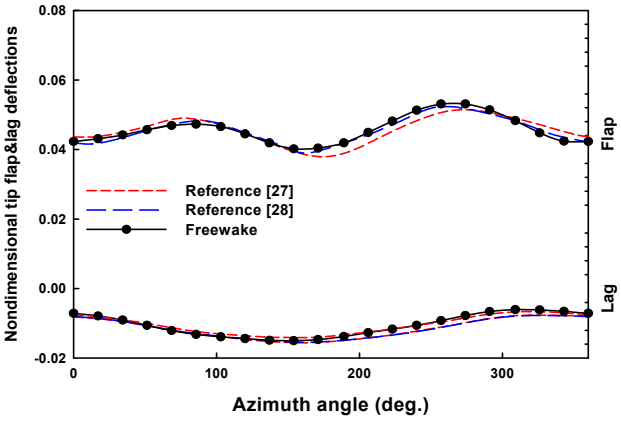

Fig.6 Periodic tip deflections
($\mu = 0.3$, $C_T/\sigma = 0.07$)

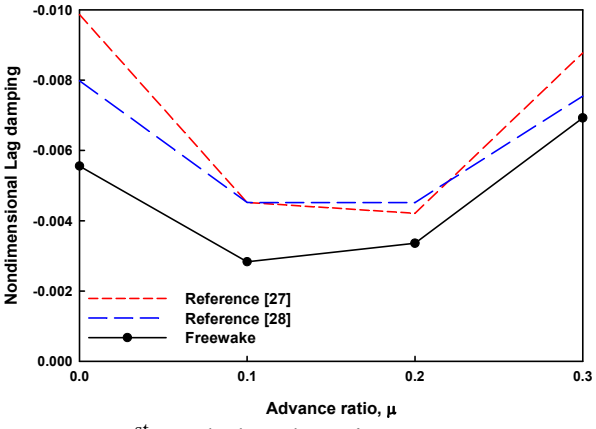

Fig.7 1st mode lag damping ($C_T/\sigma = 0.07$)

Fig. 7 shows the variation of lag mode damping with advance ratio of 0, 0.1, 0.2 and 0.3. The present results are obtained using the Floquet theory with the modal basis. The results obtained from freewake model were compared

with those obtained from Ref. [27, 28]. However, it shows some differences between the results of two models in hover condition, and the differences increase as the forward speed increases. The full finite element analysis using the large deflection beam theory and freewake method gives lower values in the lag mode damping due to the different structural and aerodynamic approaches.

4 Conclusions

In this study, aeroelastic analyses of helicopter rotor blades in hover and forward flight were presented. The large deflection beam model was applied to structural modeling with consideration of the nonlinear behaviors of the blades. Also, the freewake model was employed as a means of considering the wake effects. The stability analyses were performed and the damping and frequencies in lag modes were investigated and verified experimentally. The damping which related with aeroelastic instability was significantly affected by the wake effects. Furthermore, the lag damping values derived from the freewake model were coincided with experimental results but were smaller than the results derived from the two-dimensional quasi-steady model. In the final analysis, this study will be helpful to investigate aeroelastic characteristics of blades in the rotor design stage.

Acknowledgement

This paper was supported by Bearingless Rotor Hub System Development Program, Korea Aerospace Technology Research Association and Ministry of Knowledge and Economy (MKE), Korea and was also supported by World Class University (WCU) program through the National Research Foundation of Korea funded by the Ministry of Education, Science and Technology (R31-2008-000-10045-0).

References

[1] Johnson W. *Helicopter Theory*, Princeton University Press, Princeton, NJ, 1980.

[2] Leishman JG. *Principles of Helicopter Aerodynamics*, Cambridge University Press, New York, NY, 2000.

[3] Friedmann PP and Hodges DH. Rotary-Wing Aeroelasticity with Application to VTOL Vehicles, Flight-Vehicle Materials, Structures, and Dynamics, *American Society of Mechanic al Engineers*, New York, NY, 1993, pp. 299–391.

[4] Chopra I. Dynamic Stability of a Bearingless Circulation Control Rotor Blade in Hover, *Journal of the American Helicopter Society*, Vol. 30, No. 4, pp. 40–47, 1985.

[5] Marchman JF and Uzel JN. Effect of Several Wing Tip Modifications on a Trailing Vortex, *Journal of Aircraft*, Vol. 9, No. 9, pp. 684–686, 1972.

[6] Carpenter PJ and Friedovich B. Effect of a Rapid Blade-Pitch Increase on the Thrust and Induced-Velocity Response of a Full-Scale Helicopter Rotor, NACA TN 3044, 1953.

[7] Johnson W. A Comprehensive Analytical Model of Rotorcraft Aerodynamics and Dynamics, Part I: Analytical Development, NASA TM 81182, 1980.

[8] Sadler SG. A Method for Predicting Helicopter Wake Geometry, Wake-Induced Inflow and Wake Effects on Blade Airloads, *American Helicopter Society 27th Annual Forum Proceedings*, Washington, DC, May 1971.

[9] Brentner KS and Jones HE. Noise Prediction for Maneuvering Rotorcraft, AIAA 2000–2031, *6th AIAA/CEAS Aeroacoustics Conference Proceedings*, Lahaina, HI, June 12–14, 2000.

[10] Boeing. *Statistical summary of commercial jet airplane accidents worldwide operations 1959-2003*, 2004.

[11] Murugan S and Ganguli R. Aeroelastic stability enhancement and vibration suppression in a composite helicopter rotor, *Journal of Aircraft*, Vol. 42, No. 4, pp. 1013-1024, 2005.

[12] Xiong JJ and Yu X. Helicopter rotor-fuselage aeroelasticity modeling and solution using the partition-iteration method, *Journal of Sound and Vibration*, Vol. 302, No. 4-5, pp. 821-840, 2007.

[13] Byers L and Gandhi F. Embedded absorbers for helicopter rotor lag damping, *Journal of Sound and Vibration*, Vol. 325, No. 4-5, pp. 705-721, 2009.

[14] Friedmann PP, Glaz B and Palacios R. A moderate deflection composite helicopter rotor blade model with an improved cross-sectional analysis, *International Journal of Solids and Structures*, Vol. 46, No. 10, pp. 2186-2200, 2009.

[15] Shahverdi H, Nobari AS, Behbahani-Nejad M and Haddadpour H. Aeroelastic analysis of helicopter rotor blade in hover using an efficient reduced-order aerodynamic model. *Journal of Fluids and Structures*, Vol. 25, pp. 1243-57, 2009.

[16] Yoo SJ, Jeong MS and Lee I. Fluid-structure interaction analysis of hingeless rotor blades in hover considering wake effects. *Modern Physics Letters B*, Vol. 24, No. 13, pp. 1475-1478, 2010.

[17] Hodges DH, Dowell EH. Nonlinear equations of motion for elastic bending and torsion of twisted non-uniform rotor blades, NASA TN D-7818, 1974.
[18] Rosen A, Friedmann PP. The nonlinear behavior of elastic slender straight beams undergoing small strains and moderate rotations, *ASME Journal of Applied Mechanics*, Vol. 46, No. 1, pp. 161-168, 1979.
[19] Ganguli R and Chopra I. Aeroelastic tailoring of composite couplings and blade geometry of a helicopter rotor using optimization methods, *Journal of the American Helicopter Society*, Vol. 42, No. 3, pp. 218-228, 1997.
[20] Ganguli R. Optimum design of a helicopter rotor for low vibration using aeroelastic analysis and response surface methods, *Journal of Sound and Vibration*, Vol. 258, No. 2, pp. 327-344, 2002.
[21] Sivaneri NT and Chopra I. Dynamic stability of a rotor blade using finite element analysis, *AIAA Journal*, Vol. 20, No. 5, pp. 716-723, 1982.
[22] Fulton MV and Hodges DH. Aeroelastic stability of composite hingeless rotor blades in hover-part I: theory, *Mathematical and Computer Modeling*, Vol. 18, No. 3/4, pp. 1-17, 1993.
[23] Borri M. Helicopter rotor dynamics by finite element time approximately, *Computers and Mathematics with Applications*, Vol. 12A, No. 1, pp. 149-160, 1986.
[24] Hammond CE and Doggett RV. Determination of subcritical damping by moving-block. randomdec application, *NASA Symposium on Flutter Testing Techniques*, Oct., 1975.
[25] Müller RHG. Special vortices at a helicopter rotor blade, *Journal of the American Helicopter Society*, pp. 16-21, 1990.
[26] Kim JM, Komerath NM and Liou SG. Vorticity concentration at the edge of the inboard vortex sheet, *Journal of the American Helicopter Society*, pp. 30-34, 1994.
[27] Jeon SM. Aeroelastic analysis of composite hingeless rotor blades in hovering and forward flights, Ph.D. dissertation, KAIST, Korea, 1999.
[28] Lim JW. Aeroelastic optimization of a helicopter rotor, Ph.D. dissertation, University of Maryland, US, 1988.

Copyright Statement